A polarimetric current sensor using an orthogonally polarized dual-frequency fibre laser

1998 Meas. Sci. Technol. 9 952

(http://iopscience.iop.org/0957-0233/9/6/012)

Meas. Sci. Technol. **9** (1998) 952–959. Printed in the UK PII: S0957-0233(98)88910-8

A polarimetric current sensor using an orthogonally polarized dual-frequency fibre laser

Myung Lae Lee†, Jin Sik Park‡, Wang Joo Lee†, Seok Hyun Yun†, Yong Hee Lee† and Byoung Yoon Kim†

† Department of Physics, Korea Advanced Institute of Science and Technology, 373-1, Kusong-dong, Yusong-gu, Taejon, 305-701, South Korea
‡ Korea Telecom, Switching Technology Research Laboratory, 17, Woomyun-dong, Suhcho-gu, Seoul, 137-792, South Korea

Received 3 November 1997, in final form 9 February 1998

Abstract. We demonstrate a novel Er^{3+}-doped fibre laser operating in orthogonally polarized dual-frequency modes and its application to electric current sensing with frequency read-out. A Faraday rotating mirror and spatial hole burning effects in a gain medium and in a saturable absorber are utilized to control the lasing mode and polarization. The polarization mode beat frequency changes linearly in response to the non-reciprocal circular birefringence induced by an external magnetic field. When the laser was applied to sensing an alternating electric current with a simple phase-locked loop signal processing scheme, the slope coefficient of 8.0 kHz A_{p-p}^{-1} per turn and the noise equivalent current of 460 μA_{rms} $Hz^{-1/2}$ per turn were obtained. The new current sensor is immune to perturbations in the lead fibres.

Keywords: current sensor, laser sensor, polarimetric, fibre laser, Faraday rotation

1. Introduction

Polarimetric fibre-optic current sensors based on Ampère's law and the Faraday effect have been shown to have great potential for providing an enhanced sensitivity, wide dynamic range, elimination of high-voltage insulation and immunity from spurious electro-magnetic interference and they are of light weight and low cost. Considerable efforts to realize reliable and high-performance current sensors for industrial applications have been made [1–3].

Some of the major issues in the development of high-performance current sensors have been associated with the instabilities arising from changes in the residual birefringence of the sensing fibres due to external perturbations such as stress, vibration and temperature changes, and also from the temperature-dependent Verdet constant. The fluctuations of the polarization and intensity of the light input to the sensor due to vibration of the lead fibre have also been important sources of error. Many researchers have tackled these problems in passive polarimetric current sensors in a number of different ways [1–6], that increased the complexity of the optical configuration and electronic signal processing.

During the past few years, a new form of polarimetric sensor based on fibre lasers has been introduced for the measurement of various physical parameters [7–10]. The active polarimetric sensors have potential advantages of simplicity and frequency read-out. We have recently applied the polarimetric fibre laser sensor to current sensing using an Er^{3+}-doped fibre laser with a Faraday rotating mirror (FRM) [11]. In the demonstration, the laser operated in three longitudinal modes, one of which was polarized orthogonal to the other modes. The changes in polarization mode beat (PMB) frequency between the two eigenpolarization modes exhibited a linear relationship with the axial magnetic field produced by the electrical current. The advantages of this approach include the immunity to intensity fluctuation, freedom from lead fibre sensitivity and simplicity of electronic signal processing. Another important advantage of this approach is that the eigenpolarization modes of the laser automatically adjust themselves in the cavity in such a way that they become circularly polarized in the sensing region regardless of reciprocal external perturbations such as temperature changes and strain. This leads to a maximum sensitivity to the Faraday effect and a good stability of the slope coefficient.

In this paper, we report significant improvements and detailed characterization of the polarimetric fibre laser current sensor. We first demonstrate an Er^{3+}-doped fibre laser with the most desirable output characteristics for polarimetric sensing, namely dual-frequency and dual-

0957-0233/98/060952+08$19.50

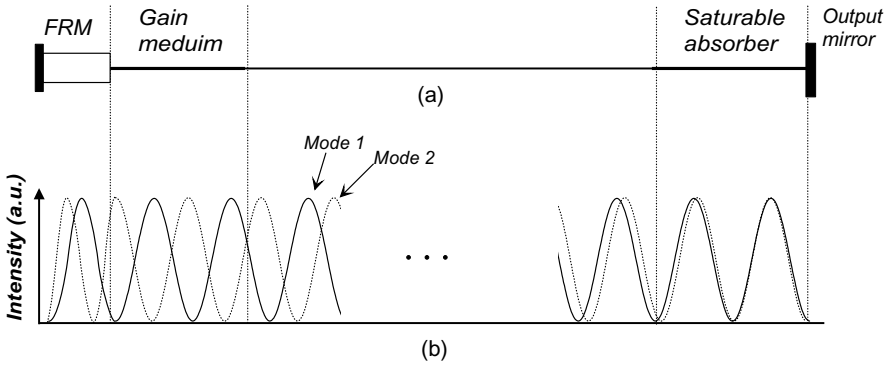

Figure 1. (a) A schematic diagram of the fibre laser cavity with a Faraday rotating mirror (FRM). (b) Standing wave patterns formed by two neighbouring frequency modes with mutually orthogonal polarization states.

polarization modes and consequently a single PMB-frequency output. This is achieved by using spatial hole burning and position control of a gain medium and a saturable absorber in the laser cavity. Secondly, the state of polarization (SOP) of the lasing modes in the laser cavity is experimentally analysed to support theoretical predictions. Some experimental results are presented, for when a fibre grating mirror, instead of a planar mirror, is used as an output mirror. Finally, we describe the performance of the current sensor employing very simple phase-locked loop (PLL) electronic signal processing scheme, for the read-out of PMB-frequency modulation. This signal processing method was not applicable to our previously demonstrated laser because of the multiple PMB frequencies of the latter [11].

2. Operating principles

2.1. The dual-frequency dual-polarization fibre laser

Figure 1(a) shows the scheme of the fibre laser consisting of a gain medium, a saturable absorber, an output planar mirror and a FRM [12] comprising a planar mirror and a 45° Faraday rotator. The gain medium and the saturable absorber that are relatively short compared with the total cavity length are positioned near the FRM and the output mirror, respectively. A polarization analysis based on the Jones matrices and the cavity resonance condition shows that the eigenpolarization modes should be circularly polarized at the output mirror and that the oscillating frequencies of the two polarization modes differ by $(N \pm \frac{1}{2})f_{FSR}$, where N is an integer and f_{FSR} is the free spectral range (FSR) of the cavity [11]. These unusual characteristics originate from the FRM acting as a conjugate mirror for the polarization state.

The principles of mode selection in the fibre laser, for a dual-frequency and -polarization output are based on spatial hole-burning effects in the gain medium and in the saturable absorber. When standing wave patterns are formed in the cavity by the intra-cavity light, they produce a gain grating in the gain medium and an absorption grating in the saturable absorber because of the intensity-dependent saturation effects in those media [13]. If frequency

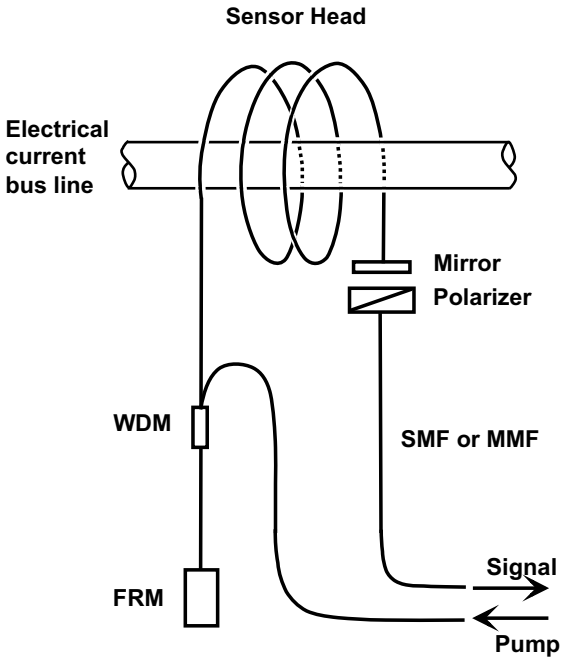

Figure 2. The configuration for a fibre laser current sensor using a fibre laser: SMF, single-mode fibre; MMF, multi-mode fibre; FRM, Faraday rotating mirror; and WDM, wavelength division multiplexer.

separations between oscillating modes in the laser are greater than the response frequency of the gain medium and the saturable absorber, the overall standing wave patterns which determine the gain or absorption gratings are a simple sum of the individual standing wave patterns formed by each mode. This condition is satisfied in our laser which utilizes Er^{3+}-doped fibres for the gain medium and the saturable absorber, since they have a response frequency of < 100 kHz while the nearest inter-modal beat frequency, $\frac{1}{2}f_{FSR}$, of the order of a few megahertz.

The visibility of the standing wave pattern formed by a particular mode at a particular point in the cavity varies depending on the eigenpolarization states and the relative intensity ratio of the two counter-propagating waves at the point. The electric field $\boldsymbol{E}_m$ of an oscillating mode m can

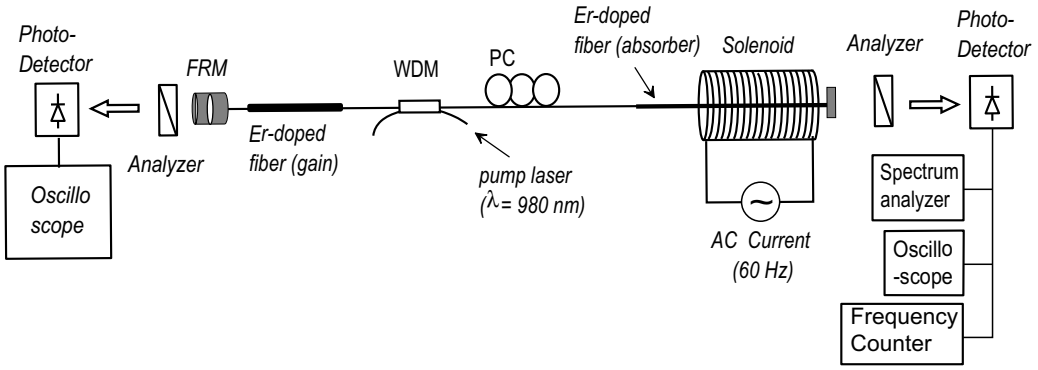

Figure 3. The experimental set-up of the fibre laser: WDM, wavelength division multiplexer; and PC, polarization controller.

be expressed as the following:

$$\boldsymbol{E}_m(z,t) = \boldsymbol{p}_m^+(z)a_m^+(z)\,\mathrm{e}^{\mathrm{i}(\beta_m z-\omega_m t)} + \boldsymbol{p}_m^-(z)a_m^-(z)\,\mathrm{e}^{\mathrm{i}(-\beta_m z-\omega_m t)} \quad (1)$$

where $\boldsymbol{p}_m^{\pm}(z)$ and $a_m^{\pm}(z)$ represent the polarization states and amplitudes of the two counter-propagating waves, respectively. The visibility of the standing wave patterns becomes

$$V_m(z) = \frac{2|a_m^+(z)||a_m^-(z)|}{|a_m^+(z)|^2 + |a_m^-(z)|^2}|\boldsymbol{p}_m^{+*}(z)\cdot\boldsymbol{p}_m^-(z)|. \quad (2)$$

In the case of a laser with a FRM,

$$\boldsymbol{p}^+(z) = \begin{pmatrix} 0 & 1 \\ -1 & 0 \end{pmatrix}\boldsymbol{p}^-(z)$$

in the Jones matrix representation based on the laboratory fixed reference frame. Thus $|\boldsymbol{p}_m^{+*}\cdot\boldsymbol{p}_m^-|$ is unity for circular polarization states and is zero for linear polarization states. In contrast, $\boldsymbol{p}^+(z) = \boldsymbol{p}^{-*}(z)$ always holds in conventional linear cavity lasers with ordinary mirrors and $|\boldsymbol{p}_m^{+*}\cdot\boldsymbol{p}_m^-|$ is unity for linear polarization states and zero for circular polarization states.

If one mode is oscillating in the laser cavity, the minimum absorption in the saturable absorber occurs at the antinodes of the standing wave pattern made by the mode. Therefore the modes whose standing wave patterns have the maximum overlap with that of the first oscillating mode will experience the minimum loss. If the saturable absorber is placed near the planar mirror, as in figure 1(a), where all standing wave patterns make a node, the nearest neighbours among the oscillating modes experience the least absorption loss. Moreover, in a fibre laser with a FRM, the eigenpolarization states are always circular at the position of the planar mirror, that ensures $|\boldsymbol{p}_m^{+*}\cdot\boldsymbol{p}_m^-| = 1$. In this case, the absorption grating acts as a narrow-bandpass filter which tends to reduce the number of oscillating longitudinal modes [14, 15].

In the gain medium, the spatial hole-burning effect leaves unused gain that can support oscillation of other modes with different standing wave patterns. The modes that get the maximum gain will be the ones whose standing wave patterns have the minimum overlap with that of the first oscillating mode inside the gain medium. The SOP of light at the FRM is a function of the birefringence

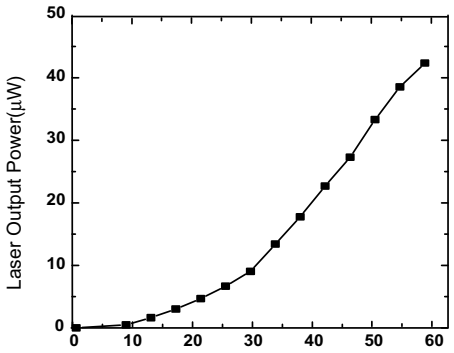

Figure 4. The laser output power versus the pump LD power from its pigtail.

of the fibre and the visibility of standing wave patterns ranges from zero for linear polarizations to unity for circular polarizations. If we consider two neighbouring longitudinal modes with mutually orthogonal circular polarization states near the FRM, their standing wave patterns are π out of phase, having the least overlap. This originates from the circular birefringence in the FRM. Together with a saturable absorber near the planar mirror, a gain medium located near the FRM provides a condition for a two-frequency laser with orthogonal polarization states.

The situation is schematically depicted in figure 1(b) for the two standing wave patterns formed by two neighbouring frequency modes in orthogonal polarization states. Note that the SOP in the saturable absorber automatically becomes circular, but that the cavity fibre birefringence has to be controlled to get circular SOPs in the gain medium. It is also assumed that the saturable absorber and the gain medium do not have significant birefringence.

Under the conditions described here, a stable oscillation of two adjacent modes can be obtained by efficiently sharing the available gain, with the help of a narrow-bandpass filter formed in the saturable absorber. Once the two modes have been made to oscillate simultaneously, an almost homogeneous gain saturation inside the gain medium leaves little room for other modes to build up. This is clearly demonstrated experimentally as described in the following sections.

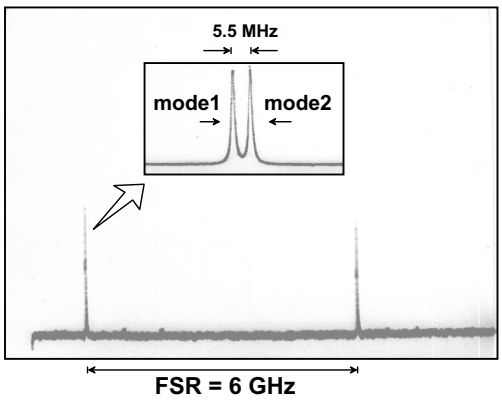

Figure 5. The output of the scanning Fabry–Pérot interferometer. A Super-Cavity Fabry–Pérot interferometer is used (FSR, 6 GHz; resolution, 1 MHz). Two modes exist.

2.2. Current sensing

When a single-mode fibre is placed in an axial magnetic field, the SOP of light propagating through the fibre experiences a circular birefringence of

$$\alpha_F = V \int_l \boldsymbol{H} \cdot \mathrm{d}\boldsymbol{l} \tag{3}$$

where V is the Verdet constant, $\boldsymbol{H}$ is the magnetic field and l is the interaction length. The Verdet constant is 7.7×10^{-7} rad A^{-1} for the fused silica at the wavelength of 1.53 μm [16].

If a magnetic field is applied to a fibre laser with a FRM when the SOP of light is circular, the induced circular birefringence introduces changes in lasing frequencies for the two circular polarization modes such that the PMB frequency f_P changes by $\Delta f_P \cong (2\alpha_F/\pi) f_{FSR}$ (when $\alpha_F \ll 1$) [11]. The factor 2 is included because the light passes through the laser cavity in both directions. In this case the PMB signal should take the form

$$I(t) = I_0 \left\{ 1 + \cos\left[2\pi \left(f_P + \frac{2\alpha_F}{\pi} f_{FSR} \right) \right] \right\} \tag{4}$$

where I_0 is the output intensity in each polarization mode and $f_P = \frac{1}{2} f_{FSR} = c/(4nL)$ (c is the speed of light, n is the refractive index of fused silica and L is the length of the laser cavity). Therefore, if an alternating magnetic field is applied, the PMB signal is frequency modulated that can be easily discriminated by using a PLL signal processing scheme.

Figure 2 shows a possible configuration for a current sensor using the fibre laser. Adopting Ampère's circuital law, the Faraday effect α_F is reduced to VNi, where N is the number of turns of fibre coils and i is the applied current. In this case, the change in PMB frequency Δf_P becomes $(NVi/\pi)[c/(nL)]$ and is proportional to the applied current i.

The pump light is fed into the gain medium via a lead fibre and a WDM. It should be mentioned that the output laser signal does not respond to the fluctuation

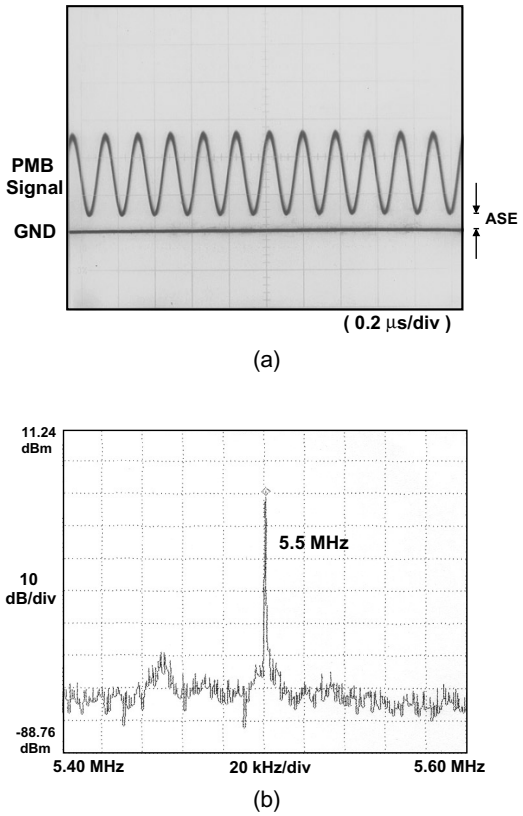

Figure 6. (a) The oscilloscope trace of the PMB and (b) its RF spectrum.

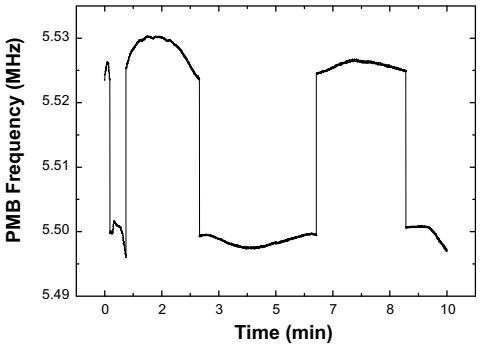

Figure 7. PMB frequency variations over 10 min. Abrupt frequency jumps are due to mode hoppings.

of the polarization of the pumping light polarization in the lead fibre, providing a significant improvement over the conventional fibre current sensors. The frequency-modulated PMB signal obtained by using a polarizer can be transmitted to a detector through a multimode or a single-mode fibre. In this sensor configuration, the frequency-encoded signals are not sensitive to the fluctuations of intensity or polarization in the lead fibres. Note that the fibre in the laser should not have significant linear birefringence in order to ensure that one has the circular SOP of light in the sensing region. One possibility is to use a circularly birefringent fibre that can be realized by twisting the fibre.

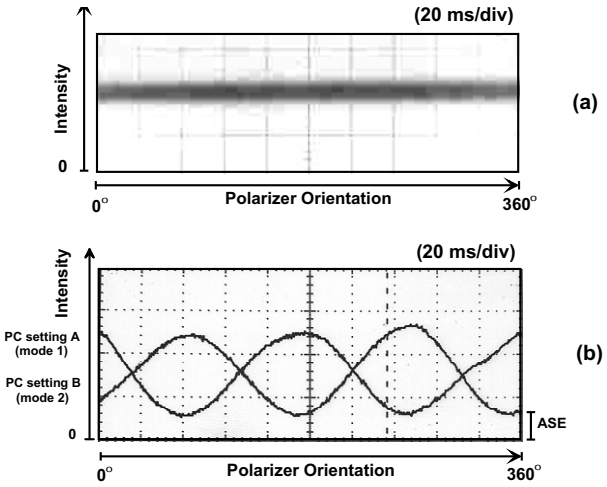

Figure 8. The intensity output from a FRM through a rotating polarizer for various PC settings: (a) when a good PMB signal was present and (b) when the PMB disappeared. Mode 1 was changed to mode 2 by adjusting the PC setting. The two modes were mutually orthogonal.

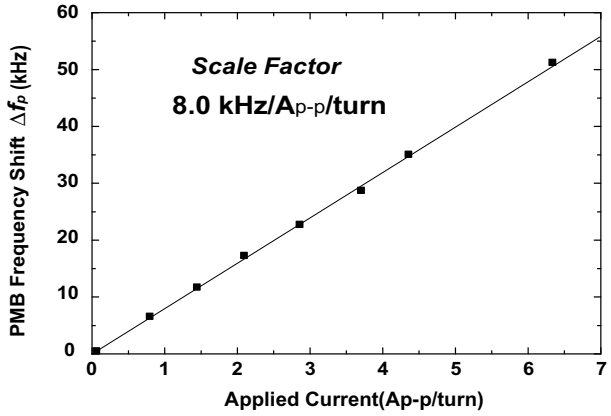

Figure 9. The slope coefficient, Δf_p A_{p-p}^{-1} per turn of the sensor.

3. Experiments

3.1. Fabrication and characterization of the fibre laser

To implement experimentally the principles of mode selection for dual-polarization and -frequency output, we constructed a fibre laser as shown in figure 3. An Er^{3+}-doped fibre (30 cm long, 2000 ppm erbium concentration) as the gain medium was spliced to a FRM (∼80% of reflectance) with a 10 cm long pigtail and pumped by a 980 nm laser diode through a WDM coupler (980/1550 nm). An unpumped Er^{3+}-doped fibre (180 cm long, 80 ppm erbium concentration and absorption coefficient of 0.664 dB m^{-1}) as a saturable absorber was butt coupled to an output planar mirror (90% of reflectance, dielectric multilayer coated). The total cavity length was about 9 m and the FSR of the cavity was about 11 MHz. A solenoid (42 cm long, 1528 turns of an electrical wire) was placed near the output planar mirror to produce a uniform axial magnetic field of a strength proportional to the applied current. The laser output from the FRM was also monitored

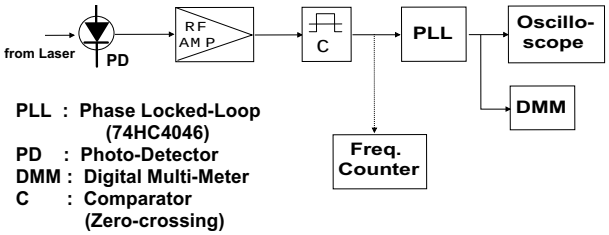

Figure 10. The block diagram of the signal processor for sensing of alternating electric current.

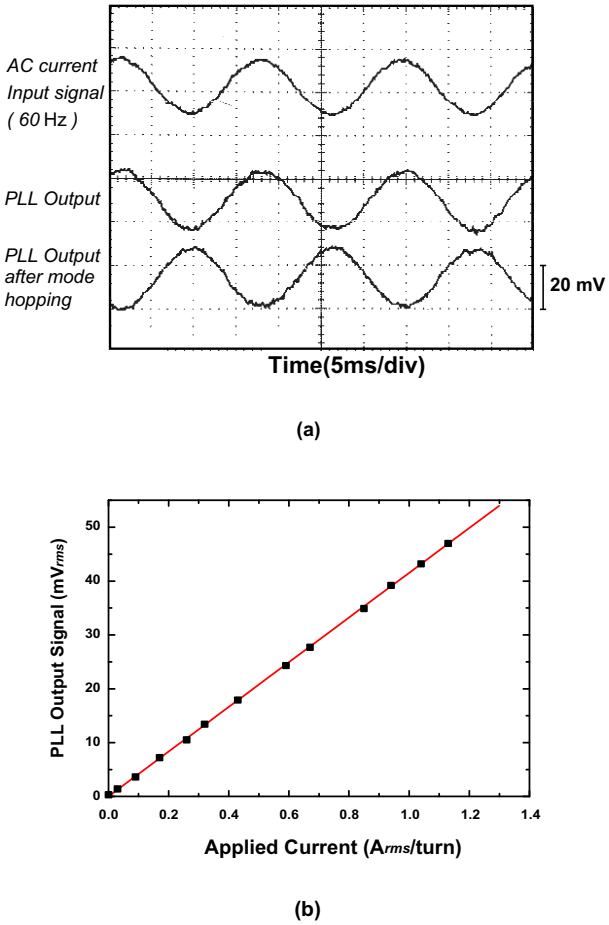

Figure 11. (a) The electrical signal applied to the solenoid (upper trace), the output of the signal processor (middle trace), and the output after a mode hop (lower trace). (b) The amplitude of the processor output as a function of that of the applied current.

for its SOP using a rotatable linear polarizer. The optical fibres in the cavity were all nominally circular-cored fibres, laid loosely on an optical bench and covered by a Plexiglass box to block the ambient air flow.

Figure 4 shows the laser output power as a function of the pump power and the gradual increase of the output power is mainly due to amplified spontaneous emission (ASE). By adjusting the polarization controller (PC), we could obtain dual-polarization and -frequency output at $\lambda \approx 1530$ nm for a pump power of between about 20 mW (the threshold pump power) and 45 mW. However, as

the pump power approached 45 mW, another mode could get sufficient gain for it to compete with the originally established modes. This mode competition caused the instability of the PMB output. The most stable PMB signal was obtained at near the threshold pump power. Figure 5 shows the output spectrum obtained with a scanning Fabry–Pérot resonator (1 MHz resolution, 6 GHz FSR), that clearly indicates that only two modes exist. The frequency separation between the two oscillating modes was about 5.5 MHz, half the FSR of the laser cavity, as expected.

Once the mode selection had been realized by a proper PC setting, it typically lasted for hours under the laboratory conditions except for occasional mode hopping for periods of a few minutes. The mode hopping took place gradually between the nearest modes when it happened. Figure 6(a) shows PMB signals produced by sending the laser output to a fast photo-detector through a polarizer and measured by an oscilloscope and an RF-spectrum analyser. The beat signal observed on an oscilloscope had a visibility of almost unity with a small DC offset owing to the background light mainly from the ASE in the gain medium. The visibility of the beat signal was independent of the orientation of the polarizer's axis, that confirmed that the two oscillating modes were mutually orthogonal and circularly polarized at the output mirror. The RF spectrum shown in figure 6(b) demonstrates that we obtained a clean PMB signal with a signal-to-noise ratio of >50 dB for a noise equivalent bandwidth of 156 Hz.

The PMB frequency was monitored using a frequency counter as illustrated in figure 7. It shows jumps due to mode hopping and slow drift within a few tens of kilohertz over a few minutes in response to fluctuations in ambient temperature. The fluctuation in frequency is due to the imperfect FRM with a polarization rotation angle deviated from 90° at the laser output wavelength [11]. The temperature dependence of the PMB frequency, however, did not cause any serious problem for the AC current sensing, as shown in the following section.

In order to determine the SOP in the gain medium, the laser output from the FRM was measured with a rotatable polarizer and a slow photo-detector (1 kHz bandwidth), while the PMB signal was monitored from the other end of the laser. When a stable PMB signal had been produced, the output intensity from the FRM was independent of the polarizer orientation, as shown in figure 8(a). This indicates that the two orthogonal polarization components were lasing. Further measurement of the PMB signal from the FRM as a function of the polarizer's orientation revealed that the SOPs of the lasing modes are circular as predicted in the previous section. When the PC was adjusted to make the PMB signal disappear, it was found that the output from the FRM was linearly polarized, as can be seen in figure 8(b). We found two PC settings, A and B, at which PMB disappeared. The SOPs of the lasing mode from these PC settings were mutually orthogonal and linearly polarized. In this case the laser oscillated with unstable multiple longitudinal modes. This observation indirectly confirms that the early arguments for the hypothesis that the mode selection process is based on gain and absorption grating formation are reasonable.

3.2. Current measurement

The fibre laser in the present set-up would not be suitable for a DC current measurement because of the drift and hopping of the PMB frequency. However, this problem can be largely tolerated in the case of an alternating current measurement.

When an AC current was applied to the solenoid, the PMB frequency changed with a slope coefficient of $\Delta f_P \simeq 8.0$ kHz $\mathrm{A}_{\mathrm{p-p}}^{-1}$ per turn, in good agreement with the theoretical value of 8.25 kHz $\mathrm{A}_{\mathrm{p-p}}^{-1}$ per turn (figure 9). The sign depends on which of the two polarization modes has the higher optical frequency. For this measurement, a RF-spectrum analyser was used and the slope coefficient is dependent on the SOP in the sensing region that is determined by the inherent birefringence of the fibre in the sensing region. The maximum slope coefficient is obtained when the SOP is circular that requires the absence of linear birefringence. Since the sensing section was a circular-cored single-mode fibre and short in length (42 cm long), the birefringence was expected to be sufficiently low to provide a stable slope coefficient. However, there was a small change in slope coefficient of about a few per cent for different settings of the PC, indicating the existence of a small linear birefringence in the sensing region. This situation can be improved by twisting the fibre to suppress the linear birefringence.

The amplitude of the alternating current is obtained simply by measuring the amplitude of the PMB frequency modulation using straightforward phase-locked loop (PLL) electronic processing. We constructed a circuit using a conventional PLL IC chip (74HC4046). The block diagram of the signal processor is shown in figure 10. The detector signal was pre-amplified and the AC component was sent to the zero-crossing comparator to produce a constant signal input to the PLL circuit. The output of the PLL represents the reproduction of the applied current that can in turn be monitored by conventional current meters. All digital processing would also be possible by using a frequency counter and a digital signal processor. In our experiment, a frequency counter was used to monitor the slow drift of the PMB frequency. Figure 11(a) shows the waveform of the applied alternating current at 60 Hz line frequency and the typical voltage output of the PLL signal processor. When mode hopping occurred, the sign of the output was reversed. Figure 11(b) shows the measured RMS value of the signal processor output as a function of that of the applied current. The stability of the sensor output against the PMB frequency drift and mode hopping with the applied current of 0.86 A_{rms} at 60 Hz was measured and is shown in figure 12. The trace for the PMB frequency exhibits random fluctuations due to the applied AC. It can be seen that the PLL output was relatively stable and was not sensitive to the PMB frequency drift and mode hopping. The noise equivalent current of the sensor was measured at the current level of 1 A_{rms} using a RF-spectrum analyser as shown in figure 13. The SNR of the signal power was about 65 dB with a noise-equivalent resolution bandwidth of 1.48 Hz. For the estimation of the SNR, the average noise level was numerically calculated from the data shown in figure 13.

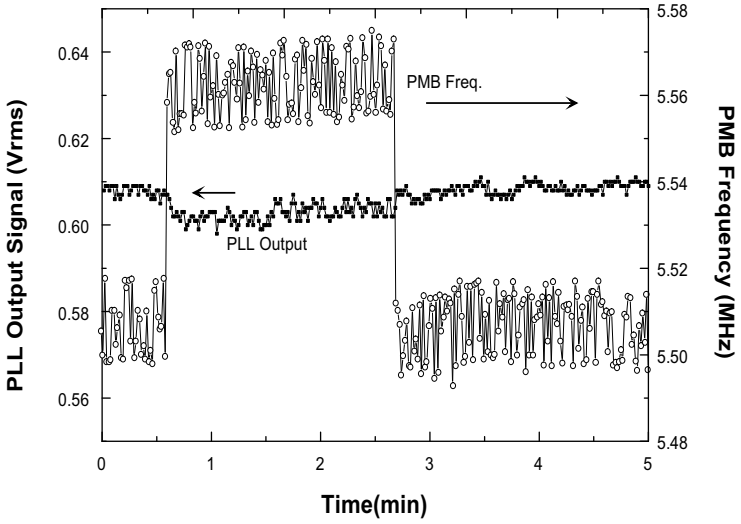

Figure 12. The stability of our set-up as a sensor against PMB drift and PLL output. The width of the PMB frequency is due to the applied current.

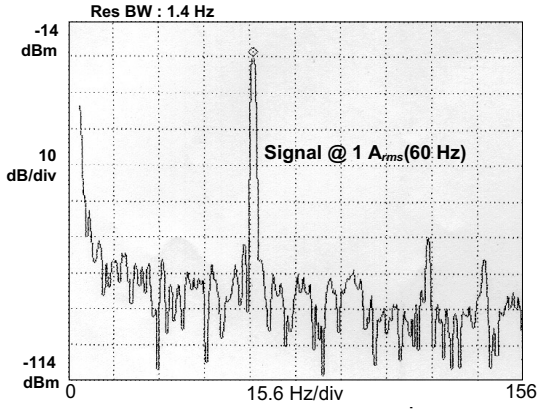

Figure 13. The RF spectrum of the signal processor output when a current of 1 A_{rms} is applied. The SNR is about 65 dB at 60 Hz line frequency with a noise-equivalent resolution bandwidth of 1.484 Hz.

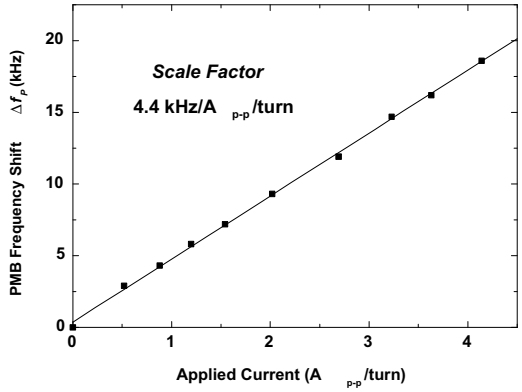

Figure 14. The slope coefficient, Δf_P A_{p-p}^{-1} per turn, when a fibre grating mirror is used to replace the planar mirror. The lower slope coefficient is due to the birefringence of the grating.

From this result we found the noise equivalent current to be about 460 μA_{rms} $Hz^{-1/2}$ per turn, which is good enough for most applications.

In an effort to achieve better modal stability, we have tried a fibre Bragg grating with a narrow reflection bandwidth instead of a planar mirror. The grating had 90% of reflectivity at 1530 nm centre wavelength with the 3 dB bandwidth of 0.5 nm. Indeed we found that the PMB signal tended to be more stable than it was in the case of a planar output mirror. However, when we measured the slope coefficient, as shown in figure 14, it was much smaller (about 55%) than the expected value. We attribute this problem to the polarization-dependent reflection properties of the fibre grating that had changed the SOP of light in the sensing region from circular to elliptical. This argument was supported by results of additional experiments using different fibre gratings that yielded vastly different slope coefficients. Further study is needed for a successful application of the fibre gratings to the fibre laser sensors.

4. Conclusions

We have demonstrated an Er^{3+}-doped fibre laser with desirable modal and polarization characteristics for a current sensor. The mode control was realized by using a FRM and a gain and an absorption grating in the laser cavity, resulting in two orthogonally polarized longitudinal modes. The SOPs of eigenmodes at the output mirror are circular polarizations. The polarization characteristics of the laser output both at the FRM and at the planar mirror were investigated.

The laser was used as an alternating electrical current sensor and the noise equivalent current was 460 μA_{rms} $Hz^{-1/2}$ per turn, using a PLL circuit as a signal processor. The frequency-modulated signal was immune to the intensity and polarization fluctuations in lead fibres. We expect the new fibre laser current sensor to offer an attractive alternative for accurate and high-performance current measurement.

Acknowledgment

This research was supported by the Agency for Defence Development of South Korea.

References

[1] Day G W, Rochford K B and Rose A H 1996 Fundamentals and problems of fiber current sensors 1996 *Proc. 11th Int. Conf. on Optical Fiber Sensors (Hokkaido, Japan, 1996)* pp 124–9

[2] Kurosawa K, Masuda I and Yamashita T 1993 Faraday effect current sensor using flint glass fiber for the sensing element *Technical Digest 9th OFS Conf., Florence* pp 415–18

[3] Tang D, Rose A H, Day G W and Etzel S M 1991 Annealing of linear birefringence in single mode fiber coils: application to optical fiber current sensors *J. Lightwave Technol.* **9** 1031–7

[4] Fang X, Wang A, May R G and Claus R O 1994 A reciprocal-compensated fiber-optic current sensor *J. Lightwave Technol.*, **12** 1882–9

[5] Pistoni N C and Martinelli M 1993 Vibration-insensitive fiber-optic current sensor *Opt. Lett.* **18** 314–16

[6] Fisher N E and Jackson D A 1996 Vibration immunity and Ampère's circuital law for a near perfect triangular Faraday current sensor *Meas. Sci. Technol.* **7** 1099–102

[7] Kim H K, Kim S K, Park H G and Kim 1993 Polarimetric fiber laser sensors *Opt. Lett.* **18** 317–19

[8] Ball G A, Meltz G and Morey W W 1993 Polarimetric heterodyning Bragg-grating fiber-laser sensor *Opt. Lett.* **18** 1976–8

[9] Kim H Y, Kim B K, Yun S H and Kim B Y 1995 Response of fiber lasers to an axial magnetic field *Opt. Lett.* **20** 1713–5

[10] Kringlebotn J T, Loh W H and Laming R I 1996 Polarimetric Er^{3+}-doped fiber distributed-feedback laser sensor for differential pressure and force measurements *Opt. Lett.* **21** 1869–71

[11] Park J S, Yun S H, Ahn S J and Kim B Y 1996 Polarization- and frequency-stable fiber laser for magnetic-field sensing *Opt. Lett.* **21** 1029–31

[12] Martinelli M 1989 A universal compensator for polarization changes induced by birefringence on a retracing beam *Opt. Commun.* **72** 341–4

[13] Siegman A E 1986 *Lasers* (Mill Valley, CA: University Science Books)

[14] Horowitz M, Daisy R, Fischer B and Zyskind J L 1994 Linewidth-narrowing mechanism in lasers by nonlinear wave mixing *Opt. Lett.* **19** 1406–8

[15] Kim H S, Kim S K and Kim B Y 1996 Longitudinal mode control in few-mode erbium-doped fiber lasers *Opt. Lett.* **21** 1144–6

[16] Noda J, Hosaka T, Sasaki Y and Ulrich R 1984 Dispersion of Verdet constant in stress-birefringent silica fiber *Electron. Lett.* **20** 906–7